ACS Macro Letters

pubs.acs.org/macroletters Letter

Elasticity of Slide-Ring Gels

Danyang Chen, Sergey Panyukov, Liel Sapir, and Michael Rubinstein*

Cite This: https://doi.org/10.1021/acsmacrolett.3c00010 Read Online

ACCESS | Metrics & More | Article Recommendations | Supporting Information

ABSTRACT: Slide-ring gels are polymer networks with cross-links that can slide along the chains. In contrast to conventional unentangled networks with cross-links fixed along the chains, the slide-ring networks are strain-softening and distribute tension much more uniformly between their strands due to the so-called "pulley effect". The sliding of cross-links also reduces the elastic modulus in comparison with the modulus of conventional networks with the same number density of cross-links and elastic strands. We develop a single-chain model to account for the redistribution of monomers between network strands of a primary chain. This model takes into account both the pulley effect and fluctuations in the number of monomers per network strand. The pulley effect leads to modulus reduction and uniform tension redistribution between network strands, while fluctuations in the number of strand monomers dominate the strain-softening, the magnitude of which decreases upon network swelling and increases upon deswelling.

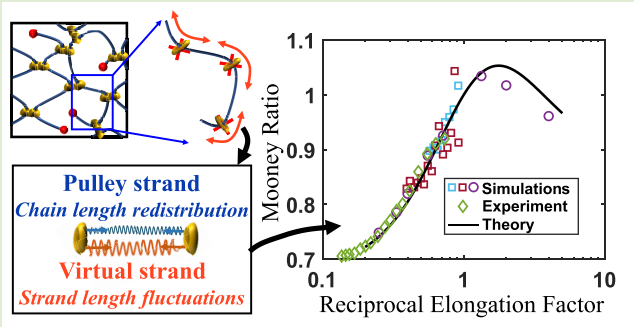

Hydrogels, which are polymer networks swollen in water, are usually very brittle and have relatively low extensibility, which limits the range of applications of these materials.[1−4] Replacing cross-links with slide-rings results in tough and stretchable hydrogels with low hysteresis.[5] The slide-rings are ring molecules (e.g., α-cyclodextrins)[6] threading on a polymer chain and can slide along the backbone (Figure 1a). The chemical cross-linking of slide-rings creates effective figure-eight structures that form a network, while still able to slide along the chains,[7] as shown in Figure 1b. The elastic modulus of slide-ring gels is lower than that of chemical gels with the same density of cross-links,[8−12] and the equilibrium swelling ratio is greater than that of equivalent cross-linked gels.[13] Slide-ring gels are capable of stretching by a much higher extension factor before failure in comparison to the typical conventional chemically cross-linked gels[11,14−18] with the same modulus (λ = 13 was reported for slide-ring gels in ref 15, while cross-linked networks with the same modulus fail at around λ = 3). The high extensibility results in a remarkably high fracture energy of ∼60 J/m^3 reported in ref 15 in comparison to the equivalent cross-linked network with fracture energy ∼10 J/m^3.

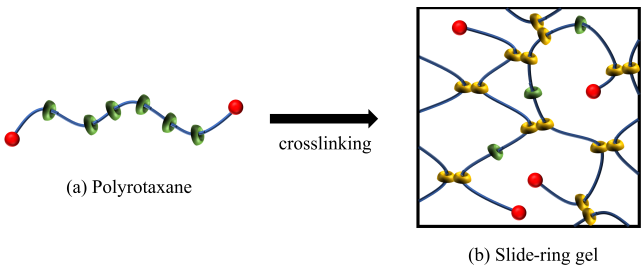

Figure 1. Schematic illustration of slide-ring gels. (a) Primary polyrotaxane chains before cross-linking. The green rings represent ring molecules that can slide along the polymer. The red beads at chain ends represent bulky end groups that prevent the rings from sliding off the chain. The rings can slide along the chain, but they cannot pass through each other. (b) In the cross-linking procedure, the rings are randomly connected in pairs to form figure-eight sliding cross-link structures (yellow pairs of rings). Free rings are shown in green. Increasing the number of free rings limits sliding and drives the properties of slide-ring gels closer to those of gels with fixed cross-links.

The study of molecular models of slide-ring gels is also an important step toward the development of the theory of topological entanglements, given the recent discovery that entangled gels also exhibit high extensibility and toughness.[19] Entanglements in polymer networks have been modeled in two different ways: either using the confining mean-field potential that restricts monomer fluctuations to a tube-like region[20−22] (collective entanglements, Figure 2a) or using discrete pairwise topological interactions[23−25] between chains (pairwise entanglements or slip-links, Figure 2b), which represent the

Received: January 5, 2023
Accepted: February 16, 2023

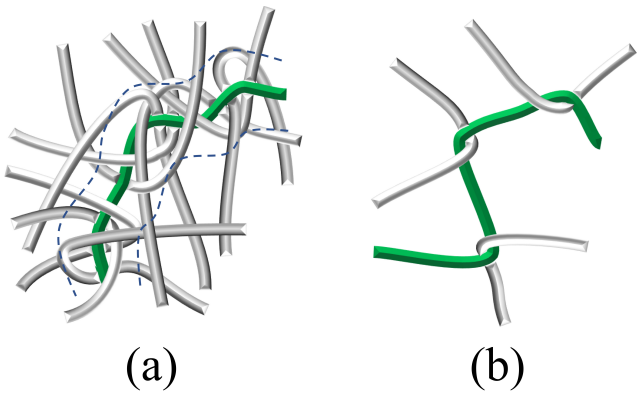

Figure 2. Schematic illustrations of (a) collective entanglements with confining tube indicated by dashed lines and (b) pairwise entanglements.

uncrossability constraints between pairs of chains. The number of pairwise topological constraints does not change with the deformation. Therefore, these pairwise entanglements can be considered as effective cross-links that can slide along the chains upon network deformation, similarly to slide-rings.

The quantitative understanding of the elasticity of slide-ring gels is still an open question. The pulley effect was taken into account in the three-chain model,[9] which assumes that each network strand can be represented by three independent substrands, respectively, along x, y, and z directions. The strand length is redistributed upon network deformation between these three substrands to minimize the total free energy. The problem with this model is that it predicts a zero elastic modulus of slide-ring gels. As shown in the modified three-chain model,[26] the elastic modulus becomes finite if an additional entropy of free rings is taken into account but is still equal to zero if all rings are cross-linked. An empirical parameter was later introduced into the three-chain model[12] to reproduce the observed reduction in the elastic modulus due to chain length redistribution. However, it remains unclear what determines this phenomenologically introduced sliding parameter. The slip-link model,[23,27−30] which was originally developed to describe entangled polymer networks, has also been used to describe slide-ring gels. Simulations of the slip-link networks have been carried out, and it has been observed that slip-link networks with end-linked primary chains show weaker strain-softening compared to randomly cross-linked slip-link networks. The original slip-link network theory[23] relies on a phenomenological parameter that determines the slidable range of slip-links. The elastic modulus was calculated using the recently proposed single-chain slip-link model.[28] In this letter, we extend this model to deformed slide-ring gels and test our predictions with molecular dynamics simulations. This multichain simulation model (section 7 in the Supporting Information) accounts for the slippage of chains through slide-rings and the spatial fluctuation of rings in space. We develop an approximate analytical solution of this multichain slide-ring model by deriving an exact solution of the affine slide-ring model (ASR) where the spatial fluctuations are ignored. We show that, in this model, the two main new effects of the slide-rings can be represented by two strands (pulley and virtual) connected in parallel. The effect of slide-ring fluctuations in space is taken into account similarly to the affine-to-phantom correction of classical cross-linked networks by multiplying the modulus of affine gel by the factor $(f - 2)/f$, with the functionality of cross-links $f = 4$. We provide the theoretical predictions for the elasticity by the phantom slide-ring (PSR) model in the case of uniaxial stretching and swelling/deswelling and compared them with molecular dynamics simulations and experiments.

The ASR model ignores spatial fluctuation of rings and is based on the following main assumptions. (i) The figure-eight slide-rings are considered to be attached to a nonfluctuating elastic background, and their positions are displaced affinely with macroscopic deformations of the gel (Figure 3b), similar to the cross-links of the classical affine network model.[31] We

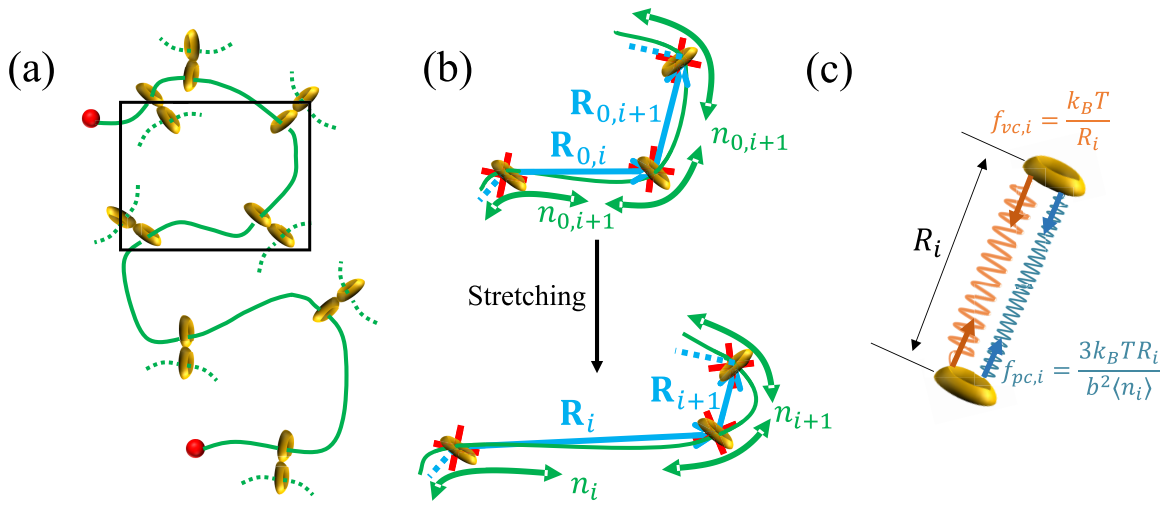

Figure 3. (a) Primary polymer chain of the slide-ring gel consisting of $q \gg 1$ network strands (chain sections between neighboring slide-rings that are parts of figure-eight cross-links). (b) Two consequent network strands in the affine slide-ring (ASR) model under preparation conditions (top) and in the uniaxially deformed network (bottom). End-to-end (ring-to-ring) strand vector (blue arrows) change under network deformation: $\mathbf{R}_{0,i} \rightarrow \mathbf{R}_i$, $i = 1, ..., q$. The number n_i of monomers in a strand, $i = 1, ..., q - 1$ is fluctuating (shown by green arrows) due to the "breathing" modes of the primary chain. (c) Each network strand i between two neighboring slide-rings can be modeled as two parallel springs, with the blue and brown springs representing a pulley strand and virtual strand, respectively. The tensions in the ith pulley strand and virtual strand are denoted by $f_{pc,i}$ and $f_{vc,i}$ respectively.

https://doi.org/10.1021/acsmacrolett.3c00010
ACS Macro Lett. XXXX, XXX, XXX−XXX

ignore the spatial fluctuation of the rings and, as a consequence, the correlations between spatial fluctuations and the fluctuations of slide-ring positions along the primary chain. (ii) Slide-ring fluctuations along the primary chain are suppressed by the presence of free rings, shown in green in Figure 1b. The effect of free rings, which is ignored in the ASR model, is calculated in section 4 in the Supporting Information. The cross-linked slide-rings with a large number of free rings per network strands act as effective cross-links. (iii) Each primary chain consists of N monomers and q strands passing through $q - 1$ rings. In principle, different primary chains could have different numbers of rings to account for the polydispersity of the number of network stands per primary chain. For large q the fluctuation in this number of rings per chain is $\sim\sqrt{q-1}$ for monodisperse primary chains and is therefore expected to be small in comparison to the total number of rings $q - 1$. (iv) Prior to cross-linking, the rings are randomly distributed along the primary chain and the positions of their attachment points are determined from the condition of the Gaussian statistics of the primary chain. These attachments ensure the uncrossabilty of rings, as the sequence of the rings through which the primary chain passes is fixed under the preparation conditions. The distributions of strand lengths and ring positions under preparation conditions are calculated in section 1 in the Supporting Information. Details of the derivation of the ASR model are given in section 3 in the Supporting Information, and here we present a physical interpretation of the model. We consider two main effects that distinguish slide-ring gels from conventional cross-linked gels: the redistribution of monomers between network strands of the primary chain and the fluctuations of the number of monomers in these network strands. Each of these effects can be described by replacing the network strand with the corresponding effective chain—the pulley strand and the virtual chain, and their combined effect—by connecting these chains in parallel (see Figure 3c).

The pulley chain consists of q pulley strands and is considered as a nonfluctuating mechanical spring (e.g., an elastic band) stretched and threaded through $q - 1$ rings (producing q pulley strands) attached to the affinely deformable, nonfluctuating background—like a rope through pulleys. The redistribution of monomers of the primary chain between its strands is determined from the condition of equality of tensions f_{pc} in its pulley strands, which gives the average number of monomers $\langle n_i \rangle$ in strand i proportional to its end-to-end distance $|\mathbf{R}_i|$. From the condition $\sum_i \langle n_i \rangle = N$ we find

$$f_{pc} = 3k_BT\frac{\sum_{i=1}^{q}|\mathbf{R}_i|}{b^2N} = 3k_BT\frac{|\mathbf{R}_i|}{b^2\langle n_i\rangle} \tag{1}$$

where k_BT is the thermal energy and b is the Kuhn length. The elastic energy of a pulley chain consisting of q pulley strands is

$$E_{pc} = \frac{3k_BT\left(\sum_{i=1}^{q}|\mathbf{R}_i|\right)^2}{2Nb^2} \tag{2}$$

which is effectively the elastic energy of a free primary chain that is extended to the total end-to-end distance, which is the sum of the lengths of all its strands.

For isotropic deformation of the network upon its swelling or deswelling, all distances $|\mathbf{R}_i|$ between slide-rings change by the same factor, and the average number of monomers $\langle n_i \rangle$ in the network strands i (equal to the number of monomers in the corresponding pulley strand) does not depend on isotropic deformation (no redistribution of monomers in a pulley chain). However, for anisotropic deformation, as shown in Figure 3b, network strands directed along the axis of maximum extension are stretched more than the strands along the orthogonal directions. The longer strands pull part of the chain length through the rings from the shorter strands. The average number of monomers in network strands $\langle n_i \rangle$ is equal to the number of monomers in the corresponding pulley strand i. It increases for strands in the direction of the maximum stretching and decreases along the orthogonal directions, as shown in section 2 in the Supporting Information.

Due to the presence of "breathing" fluctuation modes of a primary chain, the number of monomers n_i in strand i is not fixed but fluctuates around $\langle n_i \rangle$, with an amplitude of order square root of the number of monomers in the strand $\sqrt{N/q}$. Such fluctuations modify the average strand tension

$$\langle f_i \rangle = 3k_BT\frac{|\mathbf{R}_i|}{b^2}\left\langle \frac{1}{n_i}\right\rangle = 3k_BT\frac{|\mathbf{R}_i|}{b^2}\left(\frac{1}{\langle n_i\rangle} + \frac{1}{l_i}\right) \tag{3}$$

In the second equality, $l_i > 0$ because the average of the reciprocal ($\langle 1/n_i \rangle$) is larger than the reciprocal of the average ($\langle 1/n_i \rangle$) due to the fluctuations of n_i, see SI 5. Thus, a network strand i between two slide-rings can be interpreted as the parallel connection of two strands, as shown in Figure 3c: the pulley strand i of the pulley chain with a nonfluctuating number of monomers $\langle n_i \rangle$ (blue spring in Figure 3c) and a virtual strand with the number of monomers l_i connecting adjacent slide rings (orange spring in Figure 3c).

Virtual strands represent the effect of fluctuations (breathing modes) of the primary chain. One-dimensional fluctuations of the number of monomers n_i of the ith strand are associated with one-dimensional motion along the chain contour and can be described by the corresponding one-dimensional Gaussian virtual strand with l_i monomers of size $b/\sqrt{3}$ each. The elastic energy of this virtual strand ($3k_BT|\mathbf{R}_i|^2/2b^2l_i$) is equal to $k_BT/2$ according to the equipartition theorem. From this relation, we find that the number of monomers of the ith virtual strand

$$l_i = 3\mathbf{R}_i^2/b^2 \tag{4}$$

varies as the square of the distance between neighboring slide rings. The entropy of the virtual strand comes from the logarithm of the partition function of the virtual strand, which is the Gaussian distribution function

$$P(\mathbf{R}_i, l_i) = \left(\frac{3}{2\pi l_i b^2}\right)^{1/2}\exp\left(-\frac{3\mathbf{R}_i^2}{2l_ib^2}\right)$$

$$\frac{S_{vc,i}}{k_B} = \ln P(\mathbf{R}_i, l_i) = -\ln|\mathbf{R}_i| + \text{const} \tag{5}$$

where we used eq 4. The free energy F of a primary chain in the affine slide-ring (ASR) model is the sum of the elastic energy of the pulley chain consisting of q pulley strands (eq 2) and the entropic part related to q virtual strands (eq 5)

$$F_{ASR} = E_{pc} - TS_{vc} = \frac{3k_BT}{2Nb^2}\left(\sum_{i=1}^{q}|\mathbf{R}_i|\right)^2 + k_BT\sum_{i=1}^{q}\ln|\mathbf{R}_i| \tag{6}$$

The expanded form of the free energy F_{ASR} of a primary chain is shown in eq S15. The free energy of the PSR model is

https://doi.org/10.1021/acsmacrolett.3c00010
ACS Macro Lett. XXXX, XXX, XXX−XXX

obtained from F_{ASR} by multiplying the first two terms in the second line of eq S15 by the affine-to-phantom factor 1/2 (see eq S27).

In the case of isotropic swelling (deswelling) of the network from the polymer volume fraction ϕ_0 to ϕ, all distances $|\mathbf{R}_i|$ in eq 6 change by the same factor $(\phi_0/\phi)^{1/3}$. The elastic modulus of the phantom slide-ring network can be obtained from the free energy eq S27 at different volume fractions ϕ with eqs S28 and S29.

$$G_{PSR} = G_{ps,0}(\phi/\phi_0)^{1/3} + G_{vs,0}(\phi/\phi_0) + k_BT\frac{\nu_0}{q}(\phi/\phi_0)^{1/3} \tag{7}$$

where ν_0 is the number density of network strands and ν_0/q is the number density of primary chains at the preparation conditions. The pulley and virtual strand moduli, defined for $q \gg 1$ under preparation conditions $\phi = \phi_0$, are respectively

$$G_{ps,0} = \frac{4}{15}k_BT\nu_0 \quad G_{vs,0} = \frac{1}{10}k_BT\nu_0 \tag{8}$$

The last term in eq 7 is equal to the modulus of a primary chain with fixed ends and no slide-rings. It is the correction term for the finite number of rings and is $\sim q$ times smaller than the first two terms in eq 7. The last term in eq 7 can be neglected if the number of slide-rings per chain is large.

The pulley strand contribution at the preparation state, $G_{ps,0}$, is smaller than the modulus of the classical phantom model $G_{phantom} = k_BT\nu_0/2$ due to the redistribution of monomers between the strands. The pulley strand contribution to the slide-ring modulus (first term in eq 7) has the same concentration ϕ dependence as the modulus of the classical affine/phantom model ($G_{phantom} = G_{affine}/2 = (1/2)k_BT\nu_0(\phi/\phi_0)^{1/3}$), since the number of monomers in each pulley strand is fixed and does not vary with isotropic deformation. For a strongly swollen network, the ratio of the virtual strand and pulley strand contributions in eq 7 becomes small as the virtual strands get softer (eq 4). Therefore, the elastic modulus of strongly swollen slide-ring gels is determined primarily by the pulley strand contribution.

The modulus of strongly deswollen slide-ring networks is higher than the modulus of phantom networks because it is dominated by the contribution of fluctuations in the number of monomers between slide-rings, and this contribution increases linearly with the volume fraction as $G \simeq k_BT\nu_0(\phi/\phi_0)$. Note that the predicted concentration dependence of the modulus of deswollen slide-ring gels is even stronger than that of the nonaffine loopy globule model of entangled networks in θ-solvent ($G \approx \phi^{7/9}$).[32]

We performed multichain bead−spring molecular dynamics simulations that allow spatial fluctuations of rings and compared the simulation results with the predictions of the phantom slide-ring (PSR) model (seesection 7 in the Supporting Information). The slide-rings are modeled as seven-membered rings that can freely slide along the bead−spring primary chains. Interactions between nonbonded beads of network strands are turned off, resulting in a gel with polymers interacting exclusively through slide-rings. The modulus obtained from the molecular dynamics simulations of the multichain slide-ring gel agree well with the PSR model, as shown in Figure 4 by a dashed line corresponding to eq 7 with the third term accounting for $q = 16$ slide rings per primary chain in simulations.

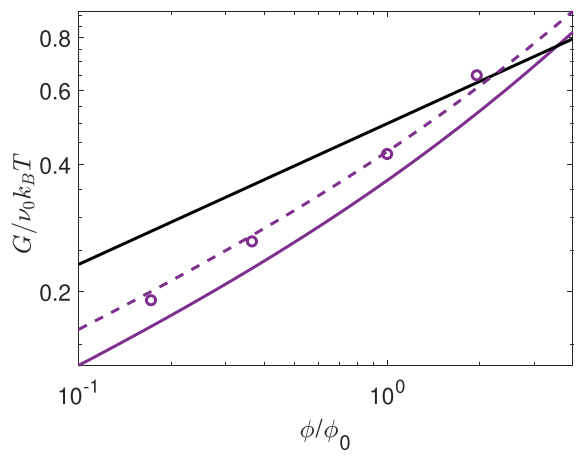

Figure 4. Elastic modulus of slide-ring gel as a function of the volume fractions normalized by the preparation volume fraction ϕ/ϕ_0. The violet circles represent the results of the multichain molecular dynamics simulations (see section 7 in the Supporting Information) with $q = 16$. The violet curve represents the prediction of the PSR model with $q = \infty$ (solid) and $q = 16$ (dashed) slide-rings (eq 7), while the solid black line depicts the phantom network model prediction.

If a slide-ring gel is uniaxially deformed at constant volume by a deformation ratio λ in the z direction, in contrast to isotropic deformation, the network strands with different orientations to the direction of uniaxial deformation are deformed differently (see section 2 in the Supporting Information). The deformation dependence of the free energy of the ASR/PSR model is significantly different from the deformation dependence of neo-Hookean free energy of the classical affine or phantom network models.[31] The number of monomers in strands of a slide-ring model increases for strands oriented in the elongation direction and decreases for strands oriented in the compression direction. The elastic stress can be obtained from the differentiation of the free energy of PSR model (eq S27) with respect to λ at $\phi = \phi_0$ (see eq S28)

$$\begin{aligned}\sigma_{PSR}(\lambda) = {} & \frac{\nu_0 k_BT}{2}\frac{1}{4\lambda(\lambda^3-1)^{5/2}}[\sqrt{\lambda^3-1}\sqrt{\lambda^3} \\ & + \ln(\sqrt{\lambda^3}+\sqrt{\lambda^3-1})][2(\lambda^3-1)^2\lambda^{3/2} \\ & + 3(\lambda^3-1)\lambda^{3/2} + (1-4\lambda^3)\sqrt{\lambda^3-1} \\ & \ln(\sqrt{\lambda^3}+\sqrt{\lambda^3-1})] + \frac{\nu_0 k_BT}{2} \\ & \frac{\sqrt{\lambda^3-1}(2\lambda^3+1) - 3\lambda^3\arctan(\sqrt{\lambda^3-1})}{2(\lambda^3-1)^{3/2}} \\ & + \frac{\nu_0 k_BT}{q}\left(\lambda^2 - \frac{1}{\lambda}\right)\end{aligned} \tag{9}$$

where the last term can be neglected for $q \gg 1$.

The deviations of the stress−strain dependence $\sigma(\lambda)$ from the neo-Hookean dependence of the affine network model $\sigma_{phantom} = \nu_0 k_BT(\lambda^2 - 1/\lambda)$ is traditionally described by the Mooney ratio[33] and shown in Figure 5a (violet circles, MD simulations of slide-ring gels, $q = 16$; violet lines, predictions of the phantom slide-ring (PSR) model, dashed line for $q = 16$ and solid line for $q = \infty$). Approximating this Mooney ratio around $\lambda = 1$ by the linear function of reciprocal elongation $\sigma/$

https://doi.org/10.1021/acsmacrolett.3c00010
ACS Macro Lett. XXXX, XXX, XXX−XXX

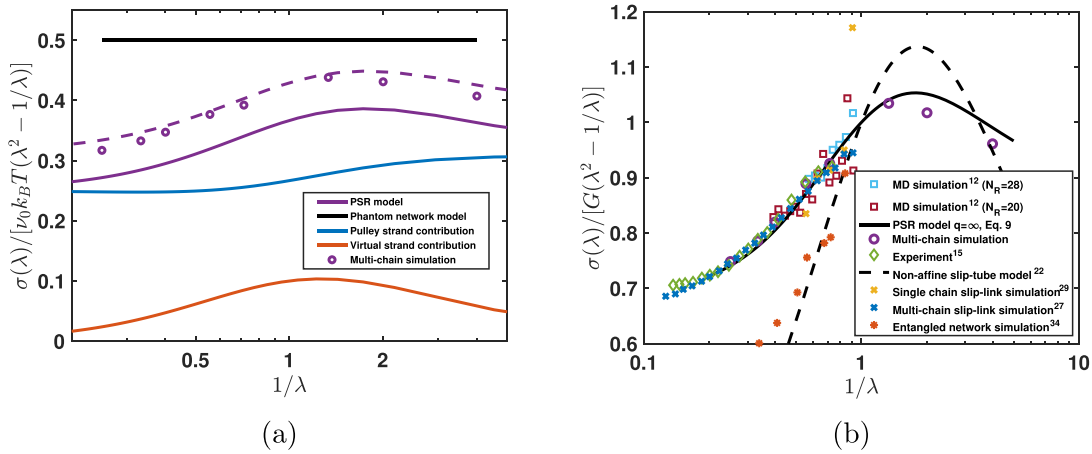

Figure 5. (a) Mooney−Rivlin plot of the ratio of stress of the slide-ring models to the neo-Hookean stress of the affine network model for the uniaxial deformation. The violet lines are the prediction of the PSR model (solid for $q = \infty$ and dashed for $q = 16$; eq 9). The pulley and virtual strand contributions are shown by blue and orange lines, respectively. The violet circles are the results of molecular dynamics simulations with $q = 16$. The black horizontal line is the prediction of the classical phantom network model. (b) Mooney dependences normalized by their values in the undeformed state. The solid curve shows the theoretical prediction of the ASR/PSR model for an infinite number of slide-rings ($q = \infty$) (eq 9). The moduli used for normalizing the curves are given in Table S1. The dashed curve shows the prediction of the nonaffine slip-tube model,[22] which describes collective entanglements (see section 8 in the Supporting Information), and the orange stars show the results of molecular dynamics simulations of entangled networks.[34]

$(\lambda^2 - 1/\lambda) = 2C_1 + 2C_2/\lambda$ for the ASR/PSR with $q = \infty$, we obtain the ratio of the Mooney coefficients, $C_2/C_1 = 2/9$, which characterizes the local strain-softening near $\lambda = 1$. The main source of strain-softening is the fact that virtual strands become softer upon stretching. As can be seen from the orange curve in Figure 5a, the virtual strands' contribution to the Mooney ratio decreases upon stretching. Figure 5b shows that the theoretical prediction of the ASR/PSR model for the nonlinear stress−strain dependence upon uniaxial deformation of slide-ring gels (black curve) agrees well not only with our multichain molecular dynamics simulations (violet circles, same as in Figure 5a), but also with other simulations[12] (blue and red squares) and experimental data[15] (green rhombuses) for slide-ring gels with a low fraction of free rings, as shown in Figure 5b. Our model also agrees well with single-chain[29] and multichain[27] slip-link simulations.

In summary, the slide-ring model presented in this work provides a very different physical picture for the slide-ring gels from previous models. Two main effects are contributing to the elasticity of the slide-ring network: (a) redistribution of chain length between network strands oriented into different directions relative to the deformation axis, which is treated as a nonfluctuating pulley chain, and (b) fluctuations of the number of monomers in network strands, which are treated as fluctuating virtual strands between rings with the number of monomers being dependent upon network deformation. The pulley effect balances the tension in all strands of the primary chain and makes slide-ring networks softer so that the pulley effect contribution to the elastic modulus is 8/15 of the modulus of cross-linked networks with the same cross-link density. However, the pulley effect does not lead to significant strain-softening upon uniaxial deformations. Fluctuations in the number of monomers per network strand add the second component, which is modeled by the virtual strands, making slide-ring gels stiffer than the network of only pulley strands. Even with strands consisting of a parallel connection of pulley and virtual chain components (Figure 3c), the slide-ring gel is still overall softer by a factor of 11/15 than a cross-linked network with the same number density of strands. This result is consistent with previous simulations[27] and predictions of the slip-link model.[28] The strain-softening behavior of slide-ring gels is dominated by the weakening of fluctuation effect upon stretching of the strands. Strongly deswollen networks, where the elasticity is dominated by the fluctuation effect, have a much stronger concentration dependence of their modulus ($G \approx \phi$) compared to cross-linked networks. This weakening of fluctuation effect upon stretching also leads to more uniform tension distribution, where the relative width of the tension distribution decreases upon swelling as $\delta f/\langle f\rangle \simeq (\phi/\phi_0)^{1/3}$ in contrast to cross-linked unentangled networks with $\delta f/\langle f\rangle \simeq$ const (section 6 in the Supporting Information). It predicts that the slide-ring gels or networks with pairwise entanglements could have strain-softening behavior even if the slide-ring positions deform affinely. The free rings (green rings in Figure 1b), that exist in the experimentally studied slide-ring gel, limit the sliding effect and lead to a weaker dependence of the Mooney ratio on deformation (see section 4 in the Supporting Information). However, they have little effect on the modulus ($(11/30)\nu k_B T$ for slide-ring gels with no free rings and $(1/3)\nu k_B T$ for slide-ring gels with many free rings per strand). There is some similarity between the slide-ring model and the slip-tube model,[22] which describes collective entanglements and includes sliding of chains along their confining tubes. Slide-ring coupling of two network strands is more analogous to pairwise rather than collective entanglements (see Figure 2). Figure 5b demonstrates that the strain-softening upon stretching in the slide-ring model is not as strong as in the slip-tube model, as it is due to the weakening of fluctuations in the number of monomers between slide-rings, rather than the softening of the confining potential. A comparison with the slip-tube model is given in section 8 in the Supporting Information, and we will present a more systematic analysis of collective and pairwise entanglements in a future publication.

https://doi.org/10.1021/acsmacrolett.3c00010
ACS Macro Lett. XXXX, XXX, XXX−XXX

■ ASSOCIATED CONTENT

Data Availability Statement

The simulation data are available at 10.7924/r4pn98b20.

Supporting Information

The Supporting Information is available free of charge at https://pubs.acs.org/doi/10.1021/acsmacrolett.3c00010.

Calculation of distribution of strand length before cross-linking, average number of monomers in network strands, calculation of the free energy of affine slide-ring model, effect of free rings, proof of inequality $\langle 1/n \rangle \geq 1/\langle n \rangle$, strand tension distributions, multichain simulation of slide-ring gel, and comparison with nonaffine slip-tube model (PDF)

■ AUTHOR INFORMATION

Corresponding Author

Michael Rubinstein − *Thomas Lord Department of Mechanical Engineering and Materials Science, Duke University, Durham, North Carolina 27708, United States; Departments of Biomedical Engineering, Chemistry, and Physics and NSF Center for the Chemistry of Molecularly Optimized Networks, Duke University, Durham, North Carolina 27708, United States; Institute for Chemical Reaction Design and Discovery (WPI-ICReDD), Hokkaido University, Sapporo 001-0021, Japan;* orcid.org/0000-0002-5455-0951; Email: michael.rubinstein@duke.edu

Authors

Danyang Chen − *Thomas Lord Department of Mechanical Engineering and Materials Science, Duke University, Durham, North Carolina 27708, United States; NSF Center for the Chemistry of Molecularly Optimized Networks, Duke University, Durham, North Carolina 27708, United States;* orcid.org/0000-0002-5622-1545

Sergey Panyukov − *P.N. Lebedev Physics Institute,, Russian Academy of Sciences, Moscow 117924, Russia; Department of Theoretical Physics, Moscow Institute of Physics and Technology, Dolgoprudny 141700, Russia;* orcid.org/0000-0003-0514-3310

Liel Sapir − *Thomas Lord Department of Mechanical Engineering and Materials Science, Duke University, Durham, North Carolina 27708, United States; NSF Center for the Chemistry of Molecularly Optimized Networks, Duke University, Durham, North Carolina 27708, United States;* orcid.org/0000-0001-7652-6541

Complete contact information is available at: https://pubs.acs.org/10.1021/acsmacrolett.3c00010

Author Contributions

CRediT: **Danyang Chen** conceptualization (equal), data curation (equal), investigation (equal), methodology (equal), writing-original draft (equal); **Sergey Panyukov** investigation (equal), methodology (equal), writing-review & editing (equal); **Liel Sapir** investigation (equal), methodology (equal), writing-review & editing (equal); **Michael Rubinstein** conceptualization (equal), funding acquisition (equal), project administration (equal), writing-review & editing (equal).

Notes

The authors declare no competing financial interest.

■ ACKNOWLEDGMENTS

This work was supported by the NSF Center for the Chemistry of Molecularly Optimized Networks (MONET), CHE-2116298, and the Institute for Chemical Reaction Design and Discovery (ICReDD) at Hokkaido University.

■ REFERENCES

(1) Gong, J.; Katsuyama, Y.; Kurokawa, T.; Osada, Y. Double-Network Hydrogels with Extremely High Mechanical Strength. *Adv. Mater.* **2003**, *15*, 1155−1158.

(2) Gong, J. P. Why are double network hydrogels so tough? *Soft Matter* **2010**, *6*, 2583.

(3) Lin, W.-C.; Fan, W.; Marcellan, A.; Hourdet, D.; Creton, C. Large Strain and Fracture Properties of Poly(dimethylacrylamide)/Silica Hybrid Hydrogels. *Macromolecules* **2010**, *43*, 2554−2563.

(4) Wang, Z.; Zheng, X.; Ouchi, T.; Kouznetsova, T. B.; Beech, H. K.; Av-Ron, S.; Matsuda, T.; Bowser, B. H.; Wang, S.; Johnson, J. A.; Kalow, J. A.; Olsen, B. D.; Gong, J. P.; Rubinstein, M.; Craig, S. L. Toughening hydrogels through force-triggered chemical reactions that lengthen polymer strands. *Science* **2021**, *374*, 193−196.

(5) Mayumi, K.; Liu, C.; Yasuda, Y.; Ito, K. Softness, Elasticity, and Toughness of Polymer Networks with Slide-Ring Cross-Links. *Gels* **2021**, *7*, 91.

(6) Okumura, Y.; Ito, K. The Polyrotaxane Gel: A Topological Gel by Figure-of-Eight Cross-links. *Adv. Mater.* **2001**, *13*, 485−487.

(7) Granick, S.; Rubinstein, M. A multitude of macromolecules. *Nat. Mater.* **2004**, *3*, 586−587.

(8) Liu, C.; Kadono, H.; Mayumi, K.; Kato, K.; Yokoyama, H.; Ito, K. Unusual Fracture Behavior of Slide-Ring Gels with Movable Cross-Links. *ACS Macro Lett.* **2017**, *6*, 1409−1413.

(9) Ito, K. Novel entropic elasticity of polymeric materials: why is slide-ring gel so soft? *Polym. J.* **2012**, *44*, 38−41.

(10) Kato, K.; Ikeda, Y.; Ito, K. Direct Determination of Cross-Link Density and Its Correlation with the Elastic Modulus of a Gel with Slidable Cross-Links. *ACS Macro Lett.* **2019**, *8*, 700−704.

(11) Ito, K. Novel Cross-Linking Concept of Polymer Network: Synthesis, Structure, and Properties of Slide-Ring Gels with Freely Movable Junctions. *Polym. J.* **2007**, *39*, 489−499.

(12) Yasuda, Y.; Masumoto, T.; Mayumi, K.; Toda, M.; Yokoyama, H.; Morita, H.; Ito, K. Molecular Dynamics Simulation and Theoretical Model of Elasticity in Slide-Ring Gels. *ACS Macro Lett.* **2020**, *9*, 1280−1285.

(13) Murakami, T.; Schmidt, B. V. K. J.; Brown, H. R.; Hawker, C. J. One-Pot "Click" Fabrication of Slide-Ring Gels. *Macromolecules* **2015**, *48*, 7774−7781.

(14) Liu, C.; Mayumi, K.; Hayashi, K.; Jiang, L.; Yokoyama, H.; Ito, K. Direct Observation of Large Deformation and Fracture Behavior at the Crack Tip of Slide-Ring Gel. *J. Electrochem. Soc.* **2019**, *166*, B3143−B3147.

(15) Jiang, L.; Liu, C.; Mayumi, K.; Kato, K.; Yokoyama, H.; Ito, K. Highly Stretchable and Instantly Recoverable Slide-Ring Gels Consisting of Enzymatically Synthesized Polyrotaxane with Low Host Coverage. *Chem. Mater.* **2018**, *30*, 5013−5019.

(16) Zhang, Z.; Hou, G.; Shen, J.; Liu, J.; Gao, Y.; Zhao, X.; Zhang, L. Designing the Slide-Ring Polymer Network with both Good Mechanical and Damping Properties via Molecular Dynamics Simulation. *Polymers* **2018**, *10*, 964.

(17) Gavrilov, A. A.; Potemkin, I. I. Adaptive structure of gels and microgels with sliding cross-links: enhanced softness, stretchability and permeability. *Soft Matter* **2018**, *14*, 5098−5105.

(18) Uehara, S.; Wang, Y.; Ootani, Y.; Ozawa, N.; Kubo, M. Molecular-Level Elucidation of a Fracture Process in Slide-Ring Gels via Coarse-Grained Molecular Dynamics Simulations. *Macromolecules* **2022**, *55*, 1946−1956.

(19) Kim, J.; Zhang, G.; Shi, M.; Suo, Z. Fracture, fatigue, and friction of polymers in which entanglements greatly outnumber cross-links. *Science* **2021**, *374*, 212−216.

(20) Edwards, S. F.; Vilgis, T. A. The tube model theory of rubber elasticity. *Rep. Prog. Phys.* **1988**, *51*, 243−297.
(21) Rubinstein, M.; Panyukov, S. Nonaffine Deformation and Elasticity of Polymer Networks. *Macromolecules* **1997**, *30*, 8036−8044.
(22) Rubinstein, M.; Panyukov, S. Elasticity of Polymer Networks. *Macromolecules* **2002**, *35*, 6670−6686.
(23) Ball, R. C.; Doi, M.; Edwards, S. F.; Warner, M. Elasticity of entangled networks. *Polymer* **1981**, *22*, 1010−1018.
(24) Rubinstein, M.; Helfand, E. Statistics of the entanglement of polymers: Concentration effects. *J. Chem. Phys.* **1985**, *82*, 2477−2483.
(25) Likhtman, A. E. Single-Chain Slip-Link Model of Entangled Polymers: Simultaneous Description of Neutron Spin-Echo, Rheology, and Diffusion. *Macromolecules* **2005**, *38*, 6128−6139.
(26) Mayumi, K.; Tezuka, M.; Bando, A.; Ito, K. Mechanics of slide-ring gels: novel entropic elasticity of a topological network formed by ring and string. *Soft Matter* **2012**, *8*, 8179.
(27) Oberdisse, J.; Ianniruberto, G.; Greco, F.; Marrucci, G. Primitive-chain Brownian simulations of entangled rubbers. *Europhysics Letters (EPL)* **2002**, *58*, 530−536.
(28) Uneyama, T.; Masubuchi, Y. Plateau Moduli of Several Single-Chain Slip-Link and Slip-Spring Models. *Macromolecules* **2021**, *54*, 1338−1353.
(29) Schneider, J.; Fleck, F.; Karimi-Varzaneh, H. A.; Müller-Plathe, F. Simulation of Elastomers by Slip-Spring Dissipative Particle Dynamics. *Macromolecules* **2021**, *54*, 5155−5166.
(30) Masubuchi, Y. Elasticity of Randomly Cross-Linked Networks in Primitive Chain Network Simulations. *Nihon Reoroji Gakkaishi* **2021**, *49*, 73−78.
(31) Wall, F. T.; Flory, P. J. Statistical Thermodynamics of Rubber Elasticity. *J. Chem. Phys.* **1951**, *19*, 1435−1439.
(32) Yamamoto, T.; Campbell, J. A.; Panyukov, S.; Rubinstein, M. Scaling Theory of Swelling and Deswelling of Polymer Networks. *Macromolecules* **2022**, *55*, 3588−3601.
(33) Mooney, M. A Theory of Large Elastic Deformation. *J. Appl. Phys.* **1940**, *11*, 582−592.
(34) Grest, G. S.; Pütz, M.; Everaers, R.; Kremer, K. Stress−strain relation of entangled polymer networks. *J. Non-Cryst. Solids* **2000**, *274*, 139−146.

https://doi.org/10.1021/acsmacrolett.3c00010
ACS Macro Lett. XXXX, XXX, XXX−XXX